

BIOLUMINESCENT ANIMAL MODELS OF HUMAN BREAST CANCER FOR TUMOR BIOMASS EVALUATION AND METASTASIS DETECTION

Liang Shan, MD, PhD; Songping Wang, PhD;
Alexandru Korotcov, PhD; Rajagopalan Sridhar, PhD;
Paul C. Wang, PhD

Introduction: Convenient animal models are needed to study the progression and treatment of human tumors *in vivo*. Luciferase-based bioluminescent imaging (BLI) enables researchers to monitor tumors noninvasively and is sensitive to subtle changes in tumors.

Methods: Three human breast cancer models in nude mice were established by using luciferase-expressing MDA-MB-231-luc cells. They were subcutaneous xenografts ($n=8$), mammary gland xenografts ($n=5$), and lung metastases ($n=3$). The tumors were imaged in live mice by using a highly sensitive BLI system. The relationship between the intensity of bioluminescence from the tumor was analyzed with respect to tumor volume. Bioluminescent signals from lung metastases were studied to determine the threshold of detectability.

Results: Tumors growing in the mice's backs and mammary gland fat pads were imaged dynamically after administration of D-luciferin. The bioluminescent intensity from the tumors gradually increased and then decreased in a one-hour span. The time to reach maximum signal intensity differed significantly among tumors and was independent of tumor volume and unrelated to maximum signal intensity. A significant correlation was observed between tumor volume and maximum signal intensity in tumors from both sites. Lung metastatic lesions of .3–.5 mm in diameter were clearly detectable through the entire animal imaging process.

Conclusion: The animal models established with luciferase-expressing cancer cells in combination with BLI provide a system for rapid, noninvasive, and quantitative analysis of tumor biomass and metastasis. This biosystem simplifies *in vivo* monitoring of tumors and will be useful for noninvasive investigation of tumor growth and response to therapy. (*Ethn Dis*. 2008;18[Suppl 2]:S2-65–S2-69)

Key Words: Bioluminescent Imaging, Luciferase, Animal Models, Breast Cancer

From the Department of Radiology (LS, SW, AK, PCW), Department of Radiation Oncology (RS), Howard University, Washington, DC.

Address correspondence and reprint requests to: Paul C. Wang, PhD; Department of Radiology, Howard University; 2041 Georgia Ave, NW; Washington, DC 20060; 202-865-3711; 202-865-3722 (fax); pwang@howard.edu

INTRODUCTION

Bioluminescent imaging (BLI) is an optical imaging modality that enables rapid *in vivo* analyses of a variety of cellular and molecular events with extreme sensitivity.^{1–3} This imaging technique is based on light-emitting enzymes, such as luciferase, as internal biological light sources that can be detected externally as biological indicators. As a result of recent developments in techniques for high-sensitivity detection of bioluminescence, BLI has been recently tested in the detection and real-time observation of primary tumor growth and metastasis in living subjects.^{4–6} Luciferase-based light-emitting animal models have also been used to develop therapeutics that target the molecular basis of disease.⁷ Importantly, BLI provides a biosystem to test the spatial-temporal expression patterns of both target and therapeutic genes in living animals where the contextual influences of whole biological systems are intact.^{8,9} In this study, we established three bioluminescent animal models of human breast cancer using MDA-MB-231-luc cell line, which has been stably transfected with the luciferase gene. The primary and metastatic lesions were analyzed through whole-animal imaging, and the tumor volume was evaluated in relationship with the bioluminescent signal intensity.

METHODS

Cell culture and animal models

MDA-MB-231-luc human breast cancer cell line and D-luciferin were obtained from Xenogen (Alameda, Calif). This cell line has been stably transfected with

luciferase gene for luciferase-based BLI. Cells were routinely maintained in Dulbecco minimal essential medium/F-12 medium supplemented with 10% heat inactivated fetal bovine serum and 50 µg/mL each penicillin, streptomycin, and neomycin (Invitrogen, Carlsbad, Calif). Female athymic nude mice of 8–10 weeks of age ($n=16$) were purchased from Harlan (Indianapolis, Ind). Three animal models were developed. The subcutaneous solid tumor xenograft model was developed by subcutaneous injection of 1×10^7 subconfluent cells in 100 µL Dulbecco phosphate buffered saline (DPBS) in the right lower back of each mouse ($n=8$). The mammary gland fat pad tumor model was developed by injection of 1×10^7 subconfluent cells in 100 µL DPBS into the right fifth mammary gland fat pad ($n=5$). Matrigel or other anchoring matrix was not used to produce the tumors. The lung metastasis model of breast cancer was developed by tail vein injection of 1×10^6 tumor cells ($n=3$). The tumors in subcutaneous tissue and mammary gland fat pad were imaged and analyzed when they reached a certain size (3–11 mm diameter). For lung metastatic model, whole animals were checked weekly and autopsied when tumor signal from the lung region was detected.

In vivo BLI

Luciferase-based BLI was performed with a highly sensitive, cooled charge-coupled device camera mounted in a light-tight specimen box (Xenogen IVIS 200 imaging system). Imaging and quantification of signals were controlled by the acquisition and analysis software Living Image (Xenogen). Mice were placed onto the warmed stage inside the light-tight camera box with continuous exposure to 2% isoflurane. After a

baseline image was taken, animals were given the substrate D-luciferin by intraperitoneal injection at 150 mg/kg in DPBS. Then the whole animal was imaged at an interval of 2 minutes for more than one hour. Imaging time was one minute. The light emitted from the mouse was detected, integrated, digitized, and displayed by the IVIS camera system. Regions of interest from the displayed images were identified and measured around the tumor sites. The signal was quantified and expressed as photons per second by using Living Imaging software (Xenogen).

All animal protocols were conducted according to National Institutes of Health guidelines for humane use and care of animals. The animal protocols were approved by the institutional animal care and use committee of Howard University.

Histopathology

To confirm whether the detected signal from whole-animal imaging originated from the metastatic lesions in the lung, the animal was autopsied as soon as the signal was detected. The lung was examined and fixed by intrabronchial perfusion of 10% neutralized formalin solution. Paraffin-embedded sections were stained using hematoxylin and eosin for microscopic evaluation.

Statistical Analysis

Statistical analysis was performed by using statistical software OriginPro 7.0 (OriginLab, Northampton, Mass). A P value $<.05$ was considered to be a significant difference between any two sets of data.

RESULTS

Individual Difference in Dynamics of Tumor Bioluminescent Signals

After inoculation of the tumor cells into the subcutaneous tissue and mammary gland fat pads of the mouse,

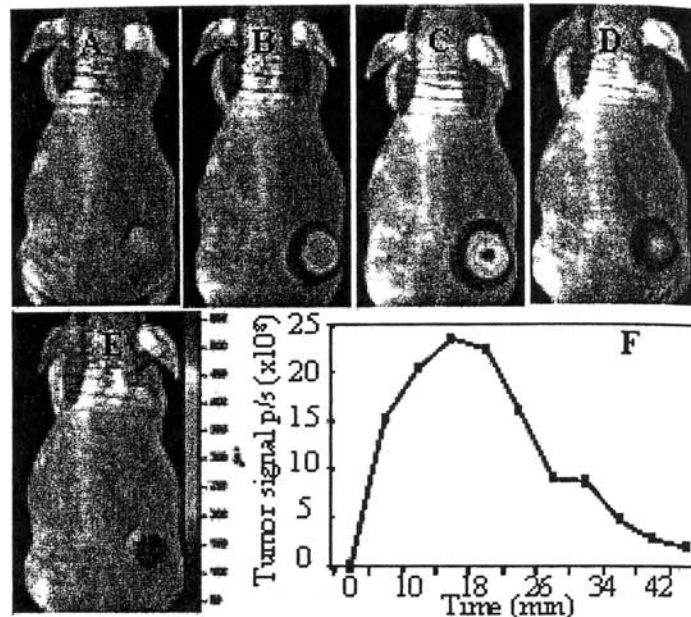


Fig 1. Dynamic change of the bioluminescent signal in tumors after administration of D-luciferin, showing gradual increase and then decrease over time. Panels A to E represent the whole animal images taken separately at 0, 10, 15, 30, and 40 minutes after luciferin administration. Panel F shows the plot of signal intensity from tumor as a function of time after injection of luciferin.

≈90% of the mice developed tumor nodules at the inoculated sites within one month. To a certain degree, the tumors varied with respect to size and rate of growth. In the present study, the tumors were allowed to grow to a desired size and used for BLI. A total of eight tumors in the subcutaneous tissue in the backs and five tumors in the mammary gland fat pads of athymic nude mice were analyzed. The maximum diameter of the 13 tumors was 3–11 mm. After administration of D-luciferin, the bioluminescent signal in tumors was clearly detectable as early as two minutes and showed a dynamic change of gradual increase and then decrease over time (Figure 1). In most of the tumors, the signal became very weak or undetectable within 60 minutes. There was a significant difference among tumors for the peak intensity time, which is defined as the time for luminescence intensity of tumor to reach the maximum, ranging from 5 to 24 minutes. A similar phenomenon

was observed for tumors located in the backs and mammary fat pads. There was no correlation between the peak intensity time and tumor volume ($R=-.13$, $P=.76$ in subcutaneous and $R=.67$, $P=.21$ in mammary gland xenografts). Also, there was no correlation between the peak intensity time and maximum tumor signal intensity ($R=-.18$, $P=.67$ in subcutaneous and $R=.74$, $P=.15$ in mammary gland xenografts). These results indicate that the dynamic change of tumor bioluminescent signal after D-luciferin administration might be related to the differences of individual mice.

Close Correlation between Bioluminescent Signal Intensity and Tumor Volume

The maximum tumor signal measured at the peak intensity time point was selected for further analysis because of the significant difference in the dynamics of tumor bioluminescent signals among mice. There was a

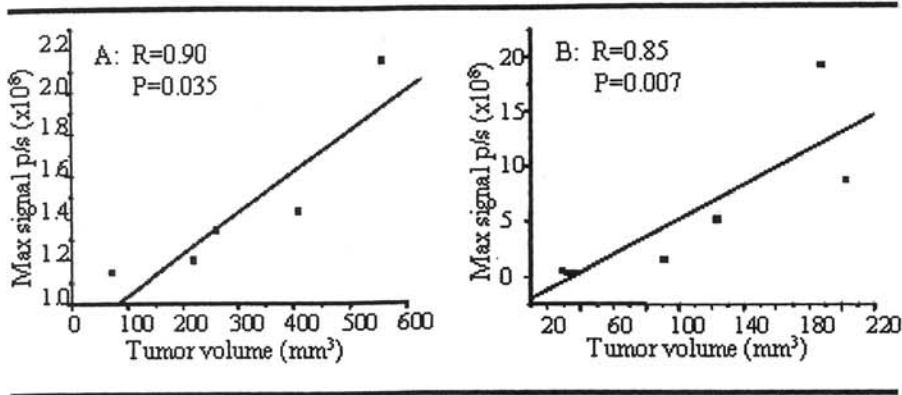


Fig 2. Close correlation between maximum signal of tumors and tumor volume. A) Solid tumor xenografts in the mammary gland fat pads of mice. B) Subcutaneous tumors in the backs of mice.

significant correlation between the maximum signal and the tumor volume for tumors located both subcutaneously ($R=.85$, $P=.007$, Figure 2B) and at the mammary gland fat pad ($R=.90$, $P=.035$, Figure 2A). This result indicates that the bioluminescent signal intensity reflects tumor size. The maximum signal intensity could be used as an indicator of tumor growth. The background signal was at a negligible level and significantly less than the signal from the tumor (Figure 1).

Highly Sensitive *in vivo* Detection of Lung Metastatic Lesions

In three mice, the tumor cells were injected through the tail vein, and whole animal imaging was performed every week. Clear signal of the tumors was first detected in the lung area at approximately one month after tail vein injection of tumor cells. After recording the images, the mice were autopsied immediately, and pathology studies of the lung were performed. In one mouse, two distinct tumor signals were observed bilaterally (Figure 3A). However, many lesions with different sizes and distributed in bilateral sides of the lung were observed under microscopy. The largest lesion located at the right lower lobe was .5 mm in diameter, corresponding to the signal on the right side

of the bioluminescent image, and the second largest lesion located at the left upper lobe was .3 mm in diameter, corresponding to the left side tumor signal in whole animal imaging (Figure 3C). In another mouse, a single tumor signal was detected, and pathology examination revealed a tumor mass of .6 mm in diameter located near the left pulmonary hilus (Figure 3B). Multiple microscopic metastatic lesions were also observed in the third mouse with very weak tumor signals. Identifying lesions <.3 mm in diameter and differ-

entiating one small lesion from another based on imaging alone was difficult.

DISCUSSION

Luciferase has served as a reporter in a number of targeted gene expression experiments in the last two decades.^{1,2} In recent years, luciferase-based BLI is becoming an important and rapidly advancing field to visualize and quantify the proliferation of tumor cells in animal models.^{10,11} Luciferase labeling is superior to other reporters, such as green fluorescent protein for tracing the progression of neoplastic growth from a few cells to extensive metastasis.^{12,13} In spite of the remarkable progress made, much more remains to be done with luciferase-based visualization of tumors *in vivo*. In the present study, we established three animal models of human breast cancer using stably luciferase-transfected cells. Regardless of the tumor sites in subcutaneous tissue or in mammary gland fat pad, the tumors could be clearly imaged with extremely low background by whole-animal imaging. Interestingly, the dynamics of the tumor signal intensity were significantly

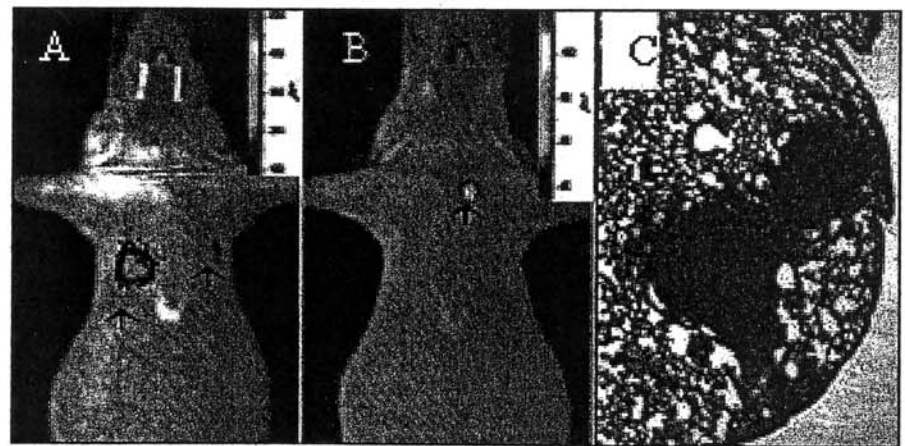


Fig 3. Detection of lung metastasis through whole animal imaging. Panel A is the image from one mouse showing signals in bilateral sides of the lung. Panel B is the image from a mouse with signal from one tumor in the left upper lobe of the lung. Panel C represents the pathologic finding of the left tumor in panel A (hematoxylin-eosin stain, $\times 40$).

different among tumors. Some tumors quickly reached the maximum intensity, whereas others took more time. The time to reach the maximum signal was independent of tumor volume and was also not related to the maximum tumor signal. There were individual differences in light emission following administration of D-luciferin. The tumor heterogeneity with respect to size, vascular density, blood supply, and other factors may affect accessibility and retention of luciferin and consequently the kinetics of light emission. Hypoxia and necrosis that are commonly observed in large tumors can lead to decreased synthesis of luciferase and ATP. The signal intensity is largely dependent on ATP and luciferase levels in the tumor and the tumor volume. In small tumors, the influence from hypoxia and necrosis may be less significant. In the present animal models, tumors <1.2 cm are more suitable for BLI because excessive necrosis was not observed under microscope. A significant correlation was observed between bioluminescent signal and tumor volume. The bioluminescent signal could be used as an indicator of tumor biomass. However, as tumors become larger, the correlation between tumor volume and bioluminescent signal becomes inferior. Another issue of concern is the selection of the time point to measure the signal intensity after luciferin administration. In the previous studies, the bioluminescent signal at the five-minute time point was arbitrarily used to represent the tumor in various analyses.^{4,5} Based on our dynamic analysis, it was clear that the signal at five-minute time point was less likely to reflect the real signal intensity of the tumors. The maximum signals at peak intensity time point may be a better indicator for tumor volume because of the strong correlation between the maximum intensity and the volume.

One potential use of BLI is the detection of metastasis in animals. The

animals can be monitored through whole-animal imaging. Wetterwald et al showed by using a bone metastasis model, that micrometastasis of .5-mm³ volume can be detected, which reveals greater sensitivity than radiographic methods.¹⁴ A study by Edinger et al using luciferase-expressing HeLa cells demonstrated that 1×10³ cells in the peritoneal cavity, 1×10⁴ cells at subcutaneous sites, and 1×10⁶ circulating cells could be observed immediately after injection of the cells.¹⁵ In the present study, clear signaling from metastatic lesions could be detected when pulmonary metastatic lesions approached .3 mm in diameter. The lesions at this stage were still difficult to differentiate from the vessel spots in magnetic resonance imaging (data not shown). All of these studies with different models confirmed the high detection sensitivity of metastatic lesions using BLI. To date, the conventional methods used to test the efficacy of novel therapies on primary tumors and metastasis *in vivo* are labor intensive and time consuming. Luciferase-based BLI is highly sensitive, real-time, noninvasive, and significantly correlated with the tumor growth. These characteristics simplify such kinds of *in vivo* analysis that rely on animals.¹⁶ The therapeutic efficacy of a drug can be assessed without having to sacrifice the mice to search for tumor growth at primary and metastatic sites. Statistically significant results can be achieved by using a small number of mice, since multiple measurements can be made over time. Although metastatic lesions above a certain critical size in the lung can be detected using BLI, a major limitation of BLI is the difficulty in quantification of multiple micrometastatic lesions and comparative analysis of lesions in different parts of the body due to the photon characteristics as well as the tissue differences along the photon pathway.

ACKNOWLEDGMENTS

This work was supported in part by DoD USAMRMC W81XWH-05-1-0291 and DAMD 17-03-1-0759, DAMD 17-03-1-0123, NIH 5U54CA091431 and grant 2G12 RR003048 from the RCMI Program, Division of Research Infrastructure, National Center for Research Resources, NIH.

REFERENCES

1. Massoud TF, Gambhir SS. Molecular imaging in living subjects: seeing fundamental biological processes in a new light. *Genes Develop.* 2003;17:545-580.
2. Greer III LF, Szalay AA. Imaging of light emission from the expression of luciferases in living cells and organisms: a review. *Luminescence.* 2002;17:43-74.
3. Yu YA, Shabahang S, Timiryasova TM, et al. Visualization of tumors and metastases in live animals with bacteria and vaccinia virus encoding light-emitting proteins. *Nat Biotech.* 2003;22:313-320.
4. Jenkins DE, Hornig YS, Oei Y, Dusich J, Purchio T. Bioluminescent human breast cancer cell lines that permit rapid and sensitive *in vivo* detection of mammary tumors and multiple metastases in immune deficient mice. *Breast Cancer Res.* 2005;7:R444-R454.
5. Nogawa M, Yuasa T, Kimura S, et al. Monitoring luciferase-labeled cancer cell growth and metastasis in different *in vivo* models. *Cancer Lett.* 2005;217:243-253.
6. Sarraf-Yazdi S, Mi J, Dewhirst MW, Clary BM. Use of *in vivo* bioluminescence imaging to predict hepatic tumor burden in mice. *J Surg Res.* 2004;120:249-255.
7. Zhang W, Moorthy B, Chen M, et al. A Cyp1a2-luciferase transgenic CD-1 mouse model: responses to aryl hydrocarbons similar to the humanized AhR mice. *Toxicol Science.* 2004;82:297-307.
8. Pilon A, Servant N, Vignon F, Balaguer P, Nicolas JC. *In vivo* bioluminescent imaging to evaluate estrogenic activities of endocrine disruptors. *Analyt Biochem.* 2005;340:295-302.
9. Vooijs M, Jonkers J, Lyons S, Berns A. Noninvasive imaging of spontaneous retinoblastoma pathway-dependent tumors in mice. *Cancer Res.* 2002;62:1862-1867.
10. Ghosh M, Gambhir SS, De A, Nowels K, Goris M, Wapnir I. Bioluminescent monitoring of NIS-mediated (131I) ablative effects in MCF-xenografts. *Mol Imaging.* 2006;5:76-84.
11. Paulmurugan R, Massoud TF, Huang J, Gambhir SS. Molecular imaging of drug-modulated protein-protein interactions in living subjects. *Cancer Res.* 2004;64:2113-2119.
12. Choy G, O'Connor S, Diehn FE, et al. Comparison of noninvasive fluorescent and

- bioluminescent small animal optical imaging. *Biotechniques*. 2003;35:1022-1026.
13. Troy T, Jelic-McMullen D, Sambucetti L, Rice B. Quantitative comparison of the sensitivity of detection of fluorescent and bioluminescent reporters in animal models. *Mol Imaging*. 2004;3:9-23.
 14. Wetterwald A, van der Pluijm G, Sijmons B, et al. Optical imaging of cancer metastasis to bone marrow: a mouse model of minimal residual disease. *Am J Pathol*. 2002;160:1143-1153.
 15. Edinger M, Sweeney TJ, Tucker AA, Olomu AB, Negrin RS, Contag CH. Noninvasive assessment of tumor cell proliferation in animal models. *Neoplasia*. 1999;1:303-310.
 16. Hardy J, Edinger M, Bachmann MH, Negrin RS, Fathman CG, Contag CH. Bioluminescence imaging of lymphocyte trafficking in vivo. *Exp Hematol*. 2001;29:1353-1360.